Materials Today: Proceedings xxx (xxxx) xxx

Contents lists available at ScienceDirect

Materials Today: Proceedings

journal homepage: www.elsevier.com/locate/matpr

Investigation of crack propagation in plain concrete using Phase-field model

Hanadi Abdulridha Lateef [a,*], Rafil Mahmood Laftah [b], Nabeel Abdulrazzaq Jasim [c]

[a] Department of Structure and Construction, Basrah Technical Institute, Southern Technical University, Iraq
[b] Department of Mechanical Engineering, Collage of Engineering, University of Basrah, Iraq
[c] Department of Civil Engineering, Collage of Engineering, University of Basrah, Iraq

ARTICLE INFO

Article history:
Available online xxxx

Keywords:
Concrete materials,
Phase-field model
Diffuse crack
Staggered solution
Fracture energy

ABSTRACT

Phase-field approach is adopted to investigate numerically the fracture behavior of the plain concrete beams under static load. Simply supported beams under three-point loads are examined. The implementation of the phase-field model is conducted within the commercial finite element software ABAQUS for two-dimensional brittle mode-I fracture problems. The phase-field model is built on the rate-independent variational principle of diffuse fracture. The implementation is based on both subroutines user element (UEL) and user material (UMAT). The elastic displacement and the fracture problem are decoupled and solved separately as a staggered solution. The main variables considered in this study are the length scale parameter, the fracture energy G_f and stability parameter K. The method is verified by comparing the results with a previous experimental study. The results have shown that the length scale parameter have high effect on the ultimate load and it depends strongly on the mesh size. It is also found that the ultimate load increases with increasing the fracture energy G_f, and the change of the parameter K seems not to affect the ultimate load value and the behavior of beams. To investigate the benefits and defects of the phase-field method, the analysis is compared with another numerical method using the eXtended Finite Element Method.

Selection and peer-review under responsibility of the scientific committee of the Third International Conference on Aspects of Materials Science and Engineering

1. Introduction

Concrete structures are full of cracks. The concrete has complicated failure mechanisms due to the multiscale and multiphase of the material. The location of crack initiation and direction of crack propagation are affected by the stress distribution. Several techniques were based on Griffith's linear elastic brittle fracture, which was modeled using the energy release rate. Essentially, once the energy release rate hits a critical value, the crack can grow or propagate further but this is not sufficient for determining curvilinear crack paths, crack kinking, and crack branching angles. In particular, such a theory is unable to predict crack initiation. These defects of the classical Griffith-type theory of brittle fracture can be overcome by variational methods based on energy minimization [1–4]. The phase-field method PFM considerably reduces the implementation complexity for fracture problems as it removes the need for numerical tracking of discontinuities in the displacement field that is the characteristic of discrete crack methods. This is accomplished by replacing the sharp discontinuities with a scalar damage phase-field that represents the diffuse crack topology, wherein the amount of diffusion is controlled by a regularization parameter [5–9]. An unbroken material is connected to broken materials by the phase-field, a scalar variable. If its value reaches one, the material is fully broken, thus both its stiffness and stress are reduced to zero. PFM was founded by Francfort and Marigo [10] who proposed a variational theory of fracture based on energy minimization principles. Bourdin et al. [11] provided a regularised formulation by introducing a length scale parameter that rendered the approach more suitable for numerical approximations. The variational formulation was further modified and extended to multi-dimensional mixed-mode dynamic brittle fractures [12,13]. The PFM for brittle fracture has been implemented in the commercial software ABAQUS via a User Element subroutine by Msekh et al. [5], which was later extended

* Corresponding author.
E-mail addresses: hanadi.ridha@stu.edu.iq (H. Abdulridha Lateef), rafil.laftah@uobasrah.edu.iq (R. Mahmood Laftah), nabeel_ali58@yahoo.com (N. Abdulrazzaq Jasim).

https://doi.org/10.1016/j.matpr.2021.12.146
2214-7853/
Selection and peer-review under responsibility of the scientific committee of the Third International Conference on Aspects of Materials Science and Engineering

by Liu et al. [14]. Molnar presented a fully functional implementation as an ABAQUS/Standard UEL of the phase-field model to study the quasi-static evolution of brittle fracture in elastic solids. The phase-field model is not sufficiently used to investigate the fracture of concrete material. Therefore, in this study, the fracture mechanics analysis using a phase-field model has been carried out to analyze plain concrete beam under three-point loads. The source codes (UEL and UMAT subroutines) for the 2-dimensional model that were used in this study were prepared by Molnar [15].

2. The Phase-field model

2.1. Variational formation of the Phase-field model

Griffith postulated that the total potential energy Π of an elastic body undergoing elastic fracture comprises the contributions of the elastic strain energy and the fracture energy in addition to the potential of external forces,

$$\Pi(u,\ \Gamma) = \Pi_e + \Pi_f + W_{ext} = \int_\Omega \psi_e d\Omega + \int_\Gamma g_C d\Gamma + W_{ext} \tag{1}$$

where u is the displacement, Π_e is the elastic strain energy, Π_f is the surface fracture energy, W_{ext} is the work done by the external forces, ψ_e is the elastic energy density and g_C is the critical fracture energy density. Ω is the domain of the body and Γ is the crack discontinuity surface [6], Fig. 1.

Phase-field modelling of fracture approximates the fracture surface integral expression introduced in Eq. (1) with a volume integral defined over the entire deformable domain Ω according to [6].

$$\int_\Gamma g_C d\Gamma \approx \int_\Omega g_C F_\Gamma(c,\ \nabla\ c) d\Omega \tag{2}$$

where $c = c(\boldsymbol{x}) \in [0, 1]\ \forall \mathbf{x} \in \Omega$ is the scalar phase field representing crack and ▽c is the gradient of damage variable.

The functional F_Γ assumes the following generic form

$$F_r(c, \nabla c)\frac{1}{c_w}\left(w(c)\frac{1}{2l_0} + 2l_0|\nabla c|^2\right) \tag{3}$$

where $l_o \in$ R (damage diffuse region) is a length scale parameter, Fig. 2, and w(c) and c_w are the generic crack geometric function and associated constant; these assume different expressions based on the type of fracture surface energy approximation used [2].

With the introduction of the crack surface density function in Eq. (3), the discrete description of a sharp crack Γ in Fig. 1 is transformed onto a diffused crack description as shown in Fig. 3 via the regularized crack functional $\Gamma_{l_o}(c)$ which is scaled by the length scale parameter lo,

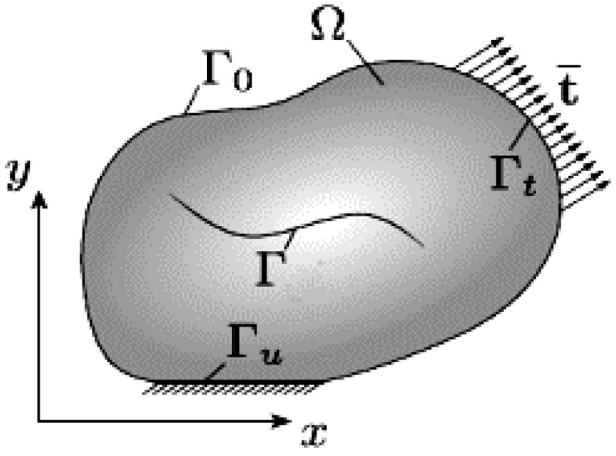

Fig. 1. Cracked Body and boundary conditions.

$$\Gamma_{l_o}(c) = \int_\Omega F_\Gamma(c, \nabla c) d\Omega \tag{4}$$

The length scale parameter l_o is the regularization length over which damage diffuses.

An exponential function was introduced to approximate the non-smooth crack topology as shown in Fig. 2 [15]:

$$c(x) = e^{-|x|/l_o} \tag{5}$$

2.2. Length scale parameter (l_o)

The length scale plays a key role in determining the phase-field approximation. l_o is introduced to facilitate the solution using numerical methods and to prevent any mesh dependence of the crack path [16,17]. The basic idea is that as the length scale approaches zero, the crack turns into the sharp crack topology as shown in Fig. 4.

The determination of l_o value is an unclear issue. Many strategies in literature were assumed by researchers. It may be considered that the length scale is chosen to be approximately more than twice the length of the smallest element size of the mesh [1,5], but this strategy is suitable for models of small dimensions only. Borden et al. (2012) and Zhang et al. (2017) as cited in Ref. [19], proposed an analytical solution for the critical tensile stress σ_{cr} that can be sustained as:

$$\sigma_{cr} = \frac{9}{16}\sqrt{\frac{EG_c}{3l_o}} \tag{6}$$

There is an apparent singularity when l_o tends to zero, i.e. in case of a sharp crack, which is physically meaningless. However, assuming all other parameters except l_o are known, Eq. (6) can be solved for l_o:

$$l_o = \frac{27EG_c}{256\sigma_{cr}^2} \tag{7}$$

where G_c is the critical energy release rate, E is modulus of elasticity and σ_{cr} is the critical stress which can be approximated by the tensile strength.

This strategy is widely accepted that the length scale l_o may be considered as a material parameter [18], but the calculated length scales yield erroneous results since they are usually too large concerning the dimensions problem. Mandal et al. in 2019 [17], assumed that the length scale l_o may be used depending on the dimensions of the model, it may be considered about one-hundredth of the largest dimension of the sample and the length scale to mesh size (h) ratio (l_o /h) equals 5–10.

In this study, the length scale is studied in two strategies: the first using Eq. (7) and the second which is assumed that the length scale depends on the sample dimensions to investigate which one is more accurate in determining the length scale.

3. Experimental beam

The beam tested by Grégoire et al. [20] is used to demonstrate the applicability of the phase-field model. The beam is subjected to three-point loads. Fig. 5 depicts the geometry, loading, and boundary conditions of the beam, the thickness of the beam is 50 mm. The notch length-to-depth of beam ratio is 0.2 and the notch width is 2 mm. The material properties parameters of concrete are listed in Table 1.

The fracture energy was not given in the Ref. [20]. Therefore, the fracture energy $\boldsymbol{G_f}$ may be estimated according to CEB- FIP MC 90 based on the compressive strength of concrete and maximum aggregate size as:

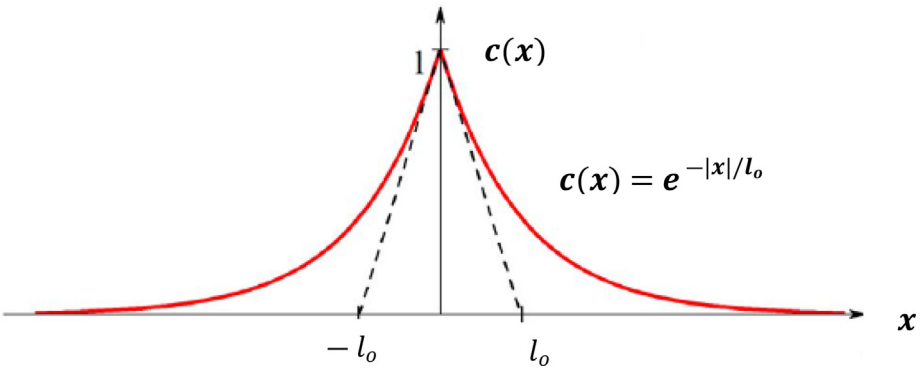

Fig. 2. Diffuse crack at x = 0 modelled with function $c(x)$ and length scale parameter l_o [15].

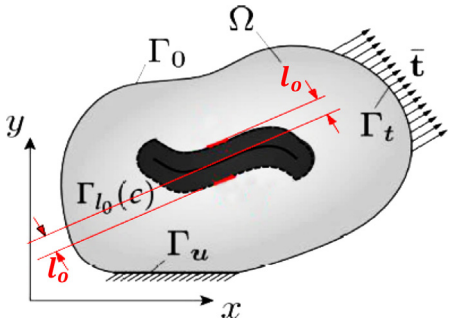

Fig. 3. The length-scale parameter l_o and boundary conditions are used to describe a diffused crack [15].

$$G_f = G_{f_0}\left(\frac{f_{cm}}{f_{cmo}}\right)^{0.7} \quad (8)$$

where, G_f is fracture energy (N/mm), G_{f_0} is the base value of fracture energy which depends on maximum aggregate size d_{max} as given in Table 2, f_{cm} is the mean value of concrete cylinder compressive strength (MPa) and f_{cmo} equals 10 MPa (constant). The fracture energy (G_f) is calculated depending on the maximum aggregate size d_{max} of 14 mm as used in the experimental test [20]. The resulting fracture energy from Eq. (8) equals 0.079 N/mm.

4. Beam modelling

The ABAQUS model of a 2-dimensional simply supported beam is shown in Fig. 6. The beam is discretized into quadrilateral elements with smaller element size at the expected crack path. Fig. 7 shows the FE mesh in which elements are in the refined zone. There are two length scale parameters are used, the first length scale value (l_o) is calculated by Eq. (7), it equals 20 mm (Model No. 1), the element size is of $h = l_o$ /10. The second length scale value is calculated at about one-hundredth of the largest dimension of the beam which becomes 2.5 mm (=250/100) (Model No. 2), the element size is of $h = l_o$ /5.

5. Analysis results and discussion

5.1. Phase-field analysis

To verify the fracture behavior of 2-dimensional beam modelled using the phase-field method, a comparison is carried out with an experimental study conducted by Grégoire et al. [20]. The stability parameter (K) is used as 0.001. The concrete material is considered isotropic and homogeneous. The details of the mesh with the length scale values are listed in Table 3.

The results of the ultimate load are presented in Table 4 for the two values of length scale parameters. Fig. 8 shows the load–deflection relationships obtained from the current study with two length scale parameters along with the experimental one [20]. The figure depicts good agreement between numerical and experimental results. The result of the phase-field model with length scale of 2.5 mm is the closest to the experimental test. The propagation of the crack for the two length scale parameters l_o at the ultimate load are shown in Fig. 9. The propagation of the crack at several load levels for model with value of l_o of 2.5 mm is shown in Fig. 10. The crack initiates at load 2.4 kN while the ultimate load is 3.72 kN.

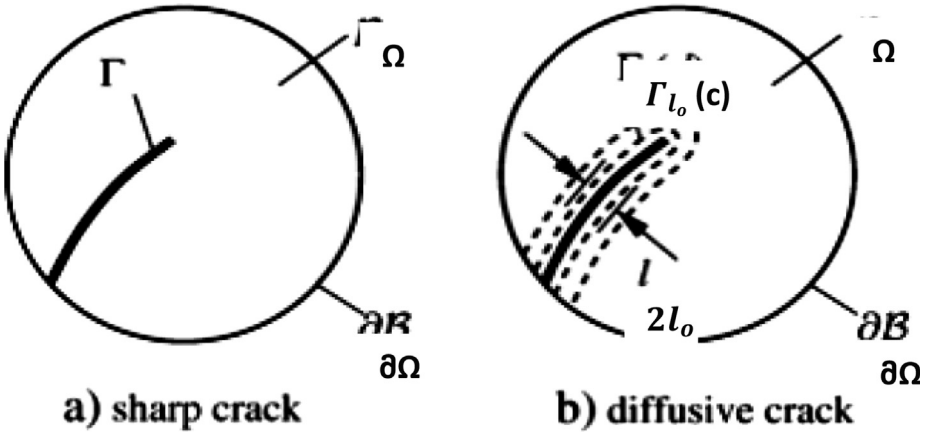

Fig. 4. Crack Topology.

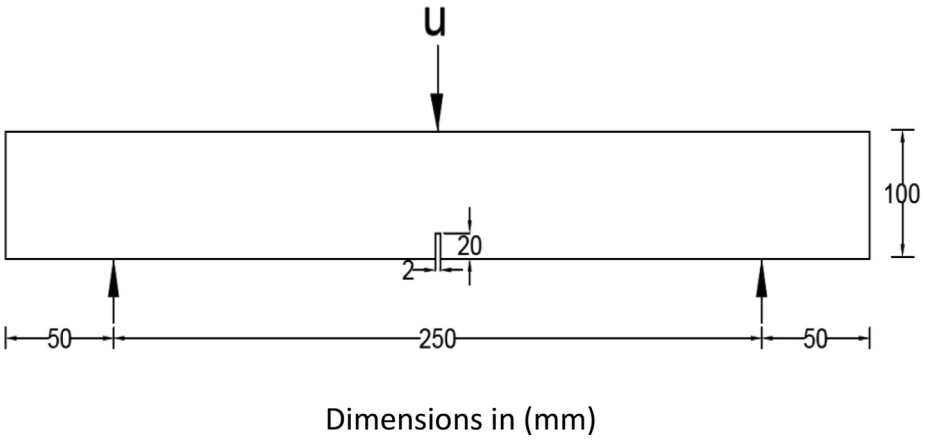

Fig. 5. Notched beam: Geometry, loading, and boundary conditions.

Table 1
The characteristics of concrete.

Compressive strength f_c (MPa)	Poisson's ratio (υ)	Modulus of elasticity E_s (GPa)	Splitting tensile strength (MPa)
42.3	0.21	37	3.9

Table 2
The base value of G_{f_0}.

d_{max} (mm)	8	16	32
G_{fo} (N/mm)	0.025	0.030	0.058

5.2. Comparison of the Phase-field method with XFEM

To emphasize the benefits and defects of the phase-field method, the analysis is compared with another numerical analysis using the eXtended Finite Element Method (XFEM).

Table 3
The length scale parameters with the smallest element size.

Model No.	Length scale l_o (mm)	Mesh size h in region l_o (mm)
1	20	2
2	2.5	0.5

The software ABAQUS is adapted to simulate the crack propagation using XFEM, taking into account materials nonlinearities using concrete damage plasticity CDP criteria. Crack initiation criteria must be specified in the XFEM. The maximum principal stress and fracture energy are very important properties in damage. The maximum principal stress damage is used with a value of the ultimate tensile strength f_t as maximum principal stress at cracking. The predefined crack was located at the mid-span of the beam with a crack length of 5 mm. The ultimate loads for two models of phase-field, experimental, XFEM and the linear strength of material approach are presented in Table 5. It seems that the PFM predicts the ultimate load more accurately than

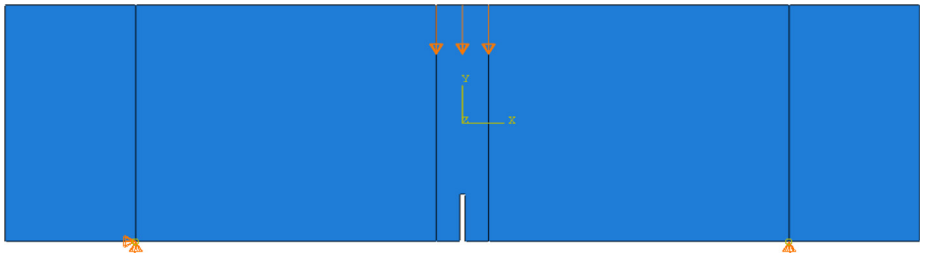

Fig. 6. The geometric setup of the beam with the loading conditions (ABAQUS model).

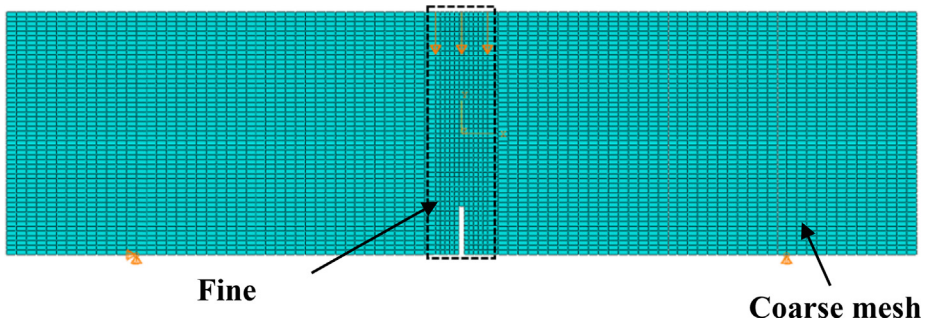

Fig. 7. Discretization of beam.

Table 4
The ultimate load for two models.

Model No.	Ultimate load (kN)	Ultimate load ratio
Experimental	3.60	1
1	3.18	0.88
2	3.72	1.03

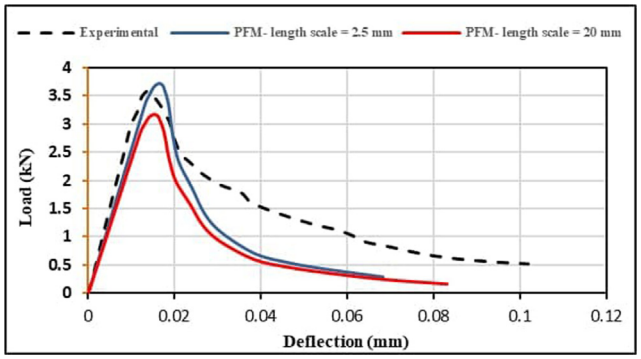

Fig. 8. Variation of mid-span deflection with load.

XFEM. However, increasing the length scale leads to understimate the ultimate load. The linear strength of material approach gives good estimate for ultimate load.

The results clearly demonstrate that the load–deflection relationships obtained from the XFE-analysis and the analysis using phase-field are in good agreement with the experimental one as shown in Fig. 11. The crack propagation using XFEM is shown in Fig. 12.

In the XFEM, the crack is included in the numerical model without modifying the discretization, as the mesh is generated without taking into account the presence of the crack. In addition, the model can be implemented with coarse mesh properly. It is also available and ready to be implmented in the ABAQUS program. The drawback of the XFEM is that it requires a predefinition of the crack and this requires more computational effort.

In the phase-field method, to capture the crack pattern properly, the mesh was refined in areas where the crack is expected to propagate. The important benefit of the phase-field method is that it does not require a predefined crack. The phase-field model is not available yet in the software programs.

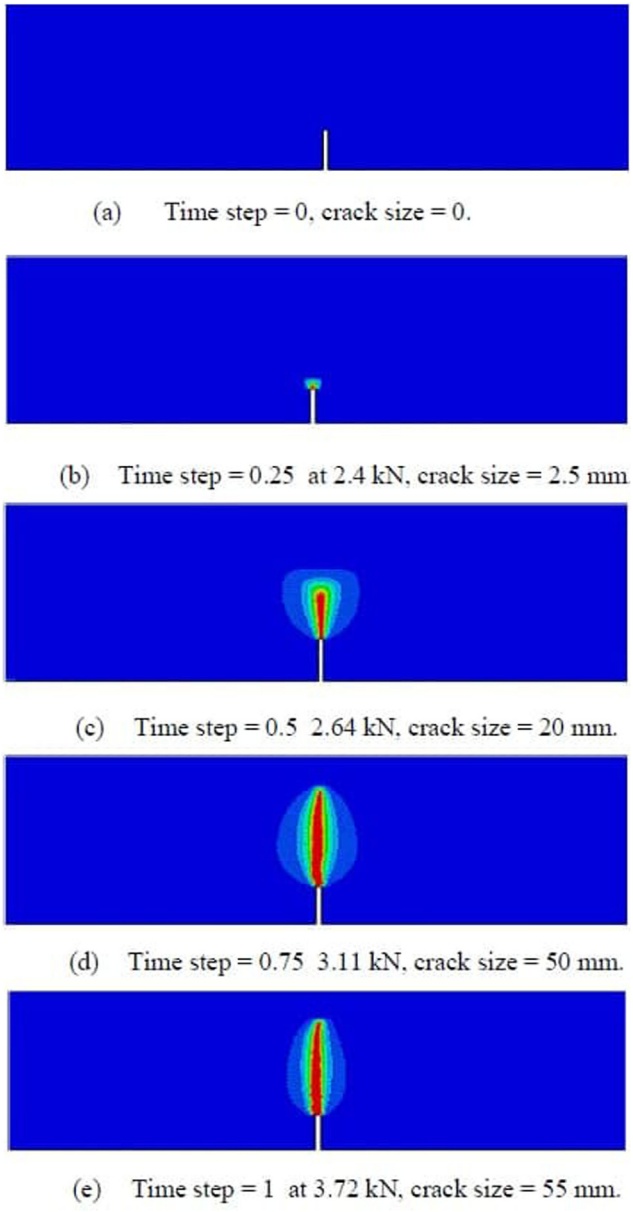

Fig. 10. The propagation of the crack at several load levels for l_o = 2.5 mm.

5.3. Investigating larger dimensions

To understand the effect of the length scale parameter clearly, larger dimensions are studied. The dimensions of the beam are 1000 mm length, 200 mm depth and the 50 mm thickness. The notch length-to-depth of beam ratio is 0.2 and the notch width is 2 mm. The material properties parameters of concrete are listed in Table 1. Three length scale parameters are studied. The first two values are calculated using the same previous strategies for the two models 1 and 2, i.e. Eq. (7) and 1/100 of larger dimensions respectively. In addition, a new value of l_o = 40 mm for Model 3 is used to investigate the larger value of the length scale (l_o). The element size is chosen as $h = l_o/10$ expect for Model 2 in which the

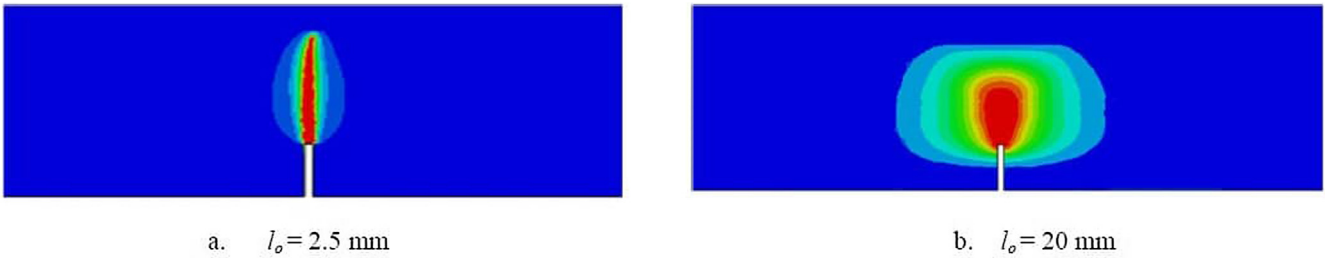

Fig. 9. The propagation of the crack: a. l_o = 2.5 mm and b. l_o = 20 mm.

Table 5
The ultimate load for two models of phase-field, experimental, XFEM and the linear strength of material.

Method	Ultimate load (kN)	Ultimate load ratio
Experimental	3.60	1
PFM-l_o = 2.5 mm	3.72	1.03
PFM-l_o = 20 mm	3.18	0.88
XFEM	3.85	1.07
Linear strength of material*	3.33	0.925

* load P = 4 M/L, M = f_t .I/y, f_t = 3.9 MPa.

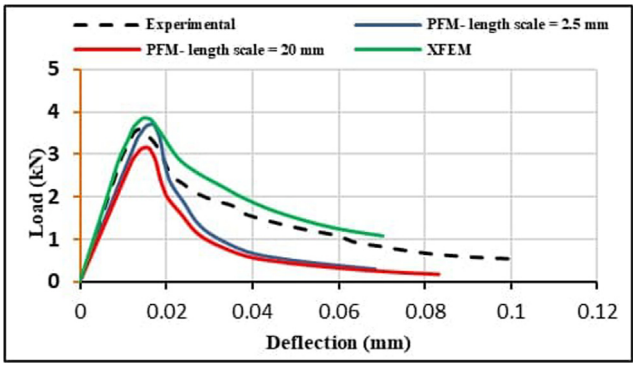

Fig. 11. Variation of mid-span deflection with load for the concrete beam using the Phase-field method and XFEM.

value l_o /5 is used as before. The details of the mesh with the length scale values are listed in Table 6.

Fig. 13 shows the load–deflection relationships for the three length scale parameters. The length scale parameter of 40 mm gives ultimate load less than those for the other l_o values. The prop-

Table 6
The length scale parameters with the smallest element size.

Model No.	Length scale l_o (mm)	Mesh size h (mm) in region l_o
1	20	2
2	10	2
3	40	4

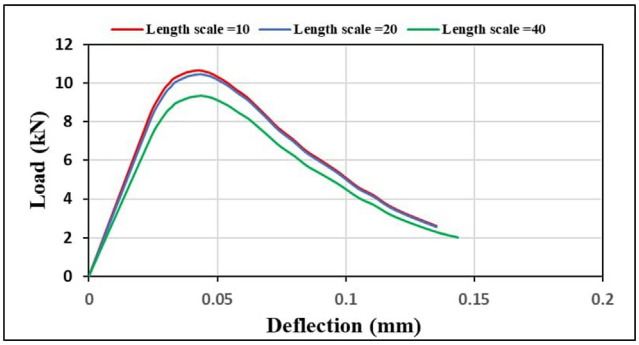

Fig. 13. Variation of mid-span deflection with load for the concrete beam.

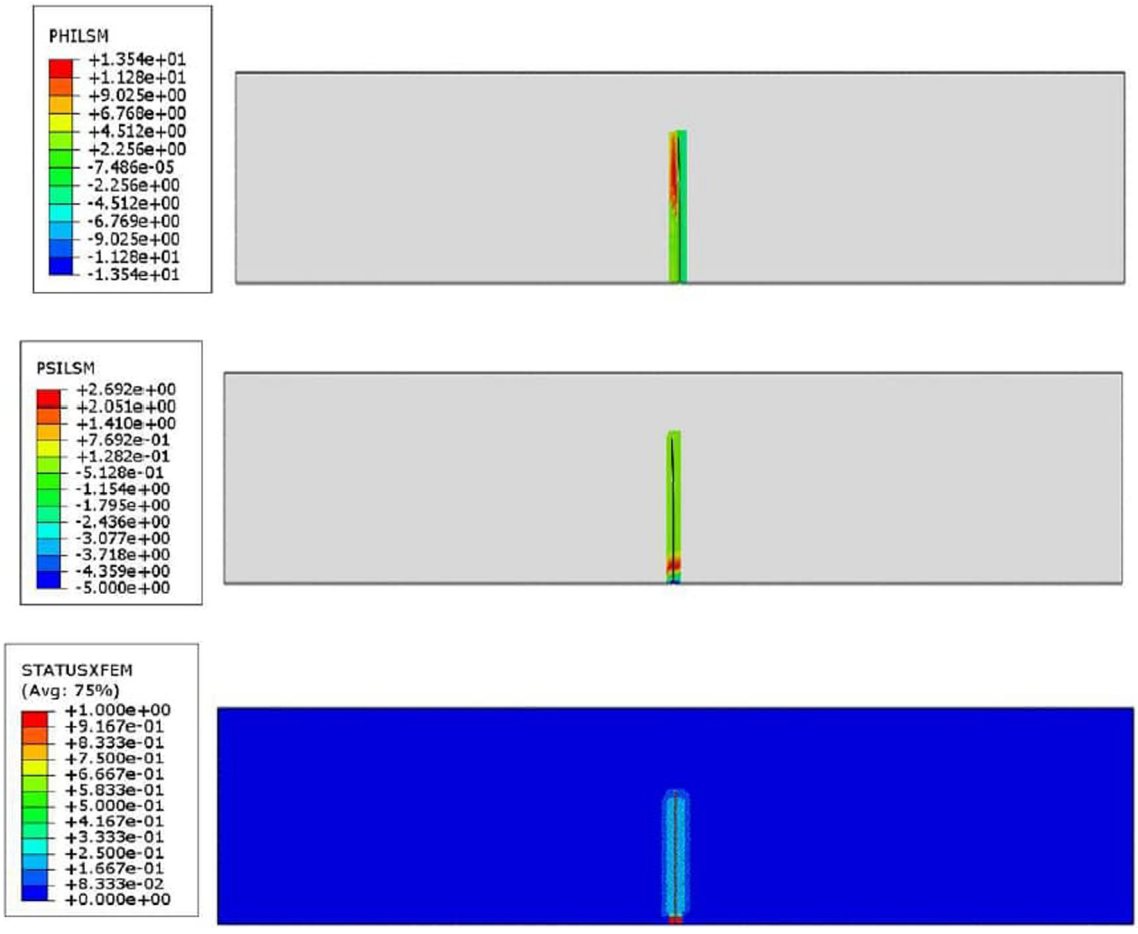

Fig. 12. Crack propagation of the concrete beam using XFEM.

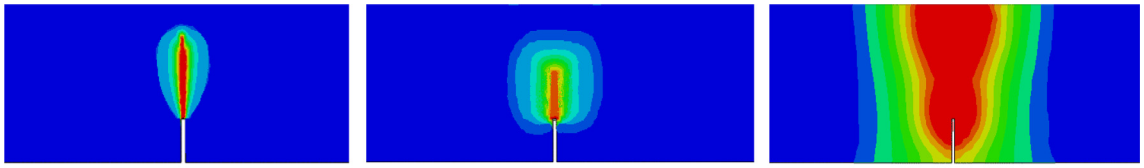

a. $l_o = 10$ mm b. $l_o = 20$ mm c. $l_o = 40$ mm

Fig. 14. The propagation of the crack for length scale: a. l_o = 10 mm, b. l_o = 20 mm and c. l_o = 40 mm (Phase-field propagation).

Table 7
The ultimate load for different values of G_f.

d_{max} (mm)	G_{fo} (N/mm)	G_f(N/mm)	G_f Ratios	Ultimate Load (kN)	Load Ratio
8	0.025	0.069	1	10.50	1
14	0.029	0.079	1.16	10.63	1.01
16	0.030	0.083	1.20	10.85	1.03
32	0.058	0.161	2.33	11.23	1.07

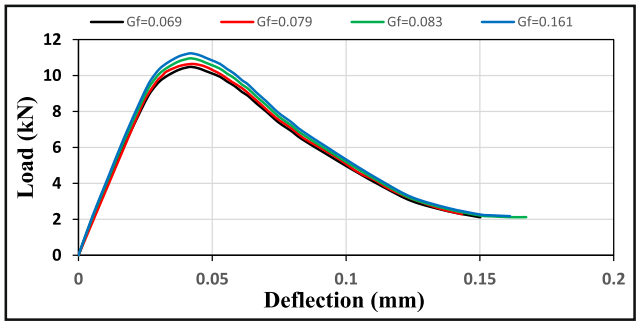

Fig. 15. Variation of mid-span deflection with load for the plain concrete beams with different fracture energies.

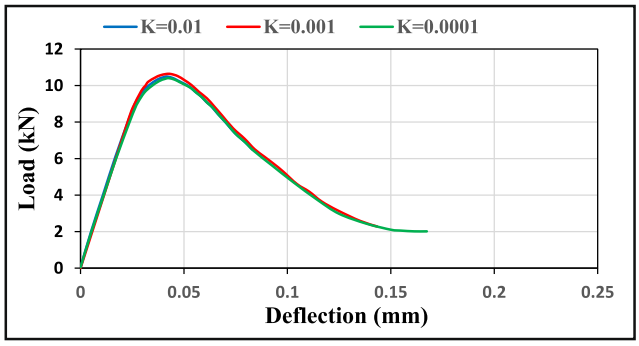

Fig. 16. Variation of mid-span deflection with load for the plain concrete beams with different stability parameters K.

agation of the crack for different length scale parameters l_o are shown in Fig. 14. Fig. 14 reveals that the value of l_o = 10 mm with element size h = 2 mm in l_o region gives the better representation of crack propagation.

5.4. Investigation of the fracture energy G_f

To understand the influence of G_f on fracture behavior of concrete beams, three beams were investigated with the same dimensions and properties, but with four different values of G_f. The used value for l_o is 10 mm and for the stability parameter (K) is 0.001.

The calculated G_f is 0.069 N/mm, 0.079 N/mm, 0.083 N/mm, and 0.161 N/mm for four sizes of aggregate, 8 mm, 14 mm, 16 mm and 32 mm, respectively. From Table 7, it is clear that the ultimate load slightly increases with increasing the G_f. The increase of G_f value by 2.33 times leads only to an increase in ultimate load by 1.07 times.

In Fig. 15, different simulations are conducted to display the effect on the load–deflection curve of different values of fracture energy. The figure illustrates also that slight increase in the toughness of the beam is obtained as a result of the increase in the fracture energy. However, the behavior of the specimens with different values of G_f is approximately the same in the first linear stage up to the initiation of the crack.

5.5. Investigation of the stability parameter K

To investigate the effect of the stability parameter Kvalue on the ultimate load, three different values of the K parameter are chosen with the fracture energy G_f of 0.079 N/mm. Fig. 16 depicts the obtained load–deflection relationships. The change of the parameter K seems not to affect the ultimate load value and the behavior of beams.

6. Conclusions

In this research, a phase-field approach is used to investigate the mechanical properties and fracture behavior of mode-I fracture of plain concrete beams. Using the phase-field approach, the crack-growth simulation was done by using a mesh that is much easier to create and does not require predefined contact surfaces to determine a crack path compared with the XFEM. To validate the phase-field approach, a comparison is carried out with an experimental study. It is clear from the results that the length scale is very important parameter in determining the crack pattern and it also affects the ultimate load value. Choosing high value of the length scale parameter gives less accurate results. Therefore, the choice of the length scale value depending on the dimensions of the model is better, because this strategy gave more acceptable results comparing to the experimental test. The formation of the crack does not mean the failure, the crack initiates at load of 2.4 kN and the ultimate load is 3.72 kN for l_o of 2.5 mm. It is also found that the ultimate load slightly increases with increasing the fracture energy G_f. An increase in value of G_f of about 2.33 times leads to increase in ultimate load of only about 7%. The change of the parameter K seems not to affect the ultimate load value and the behavior of beams. The big complaint about phase-field models is their high computational cost.

CRediT authorship contribution statement

Hanadi Abdulridha Lateef: Conceptualization, Methodology. **Rafil Mahmood Laftah:** Software, Data curation. **Nabeel Abdulrazzaq Jasim:** Writing – original draft, Visualization, Software, Investigation, Supervision, Writing – review & editing.

Declaration of Competing Interest

The authors declare that they have no known competing financial interests or personal relationships that could have appeared to influence the work reported in this paper.

References

[1] C. Miehe, M. Hofacker, F. Welschinger, A Phase Field Model for Rate-independent Crack Propagation: Robust Algorithmic Implementation based on Operator Splits, Computer Methods Appl. Mech. Eng. 199 (45-48) (2010) 2765–2778.
[2] Y.B. Zaitsev, F.H. Wittmann, Simulation of Crack Propagation, Matériaux et Construct. 14 (83) (1981) 357–365.
[3] M. Słowik, "The Analysis of Failure in Concrete and Reinforced Concrete Beams with Different Reinforcement Ratio, Conf. Arch. Appl. Mech. J., Arch. Appl. Mech. 89 (2019) 885–895.
[4] F.M. Phil, J.E. Breen, J.O. Jirsa, Concrete Fundamentals, Fifth Edition., Canada, 1988.
[5] M.A. Msekh, J.M. Sargado, M. Jamshidian, P.M. Areias, T. Rabczuk, Abaqus implementation of phase-field model for brittle fracture, Comput. Mater. Sci. 96 (2015) 472–484.
[6] A. Egger, U. Pillai, K. Agathos, E. Kakouris, E. Chatzi, I. Aschroft, S. Triantafyllou, Discrete and Phase Field Methods for Linear Elastic Fracture Mechanics: A Comparative Study and State-of-the-Art Review, Appl. Sci. 9 (2019) 2436.
[7] D.-C. Feng, J.-Y. Wu, Phase-field Regularized Cohesive Zone Model (CZM) and Size Effect of Concrete, J. Eng. Fract. Mech. 197 (2018) 66–79.
[8] C. Miehe, F. Welschinger, M. Hofacker, Thermodynamically Consistent Phase-field Models of Fracture: Variational Principles and Multi field FE Implementations, Int. J. Numer. Meth. Eng. 83 (10) (2010) 1273–1311.
[9] M. Ambati, T. Gerasimov, L. De Lorenzis, Phase- field modeling of ductile fracture, Comput. Mech. 55 (5) (2015) 1017–1040.
[10] G.A. Francfort, J.-J. Marigo, Revisiting brittle fracture as an energy minimization problem, J. Mech. Phys. Solids 46 (8) (1998) 1319–1342.
[11] B. Bourdin, G.A. Francfort, J.-J. Marigo (Eds.), The Variational Approach to Fracture, Springer Netherlands, Dordrecht, 2008.
[12] U. Farooq, K.S. Bedi, Study of Shear Behavior of RC Beams: Non-Linear Analysis, Bloomsbury Publishing India Pvt Ltd., Modeling, Simulation and Analysis, 2015, pp. 3477–3488.
[13] S.V. Chaudhari, M.A. Chakrabarti, Modeling of Concrete for Nonlinear Analysis Using Finite Element Code ABAQUS, Int. J. Comput. Applications 44 (7) (2012) 14–18.
[14] G. Liu, Q. Li, M.A. Msekh, Z. Zuo, Abaqus implementation of monolithic and staggered schemes for quasi-static and dynamic fracture phase-field model, Comput. Mater. Sci. 121 (2016) 35–47.
[15] G. Molnár, A. Gravouil, 2D and 3D Abaqus Implementation of A robust Staggered Phase-Field Solution for Modeling Brittle Fracture, J. Finite Elem. Anal. Des. 130 (2017) 27–38.
[16] I. Rašeta, A. Džolev, Đ.L. Starčev-Ćurčin, D. Kukaras, Use of Finite Element Method for Simulation of RC Beam Nonlinear Behavior, 5th Int. Conf. Contemporary Achievements Civ. Eng. (2017) 243–252.
[17] T.K. Mandal, P.V. Nguyen, J.-Y. Wu, Length scale and mesh bias sensitivity of phase-field models for brittle and cohesive fracture, Eng. Fract. Mech. 217 (August 2019) 1–29.
[18] B.A. Robertson, Phase Field Fracture Mechanics MAE 523 Term Paper, Arizona University, November 2015, pp. 1-24.
[19] S. Zhou, X. Zhuang, H. Zhu, T. Rabczuk, Phase field modelling of crack propagation, branching and coalescence in rocks, Theor. Appl. Feacture Mech. 96 (2018) 174–192.
[20] D. Grégoire, L.B. Rojas-Solano, G. Pijaudier-Cabot, Failure and size effect for notched and unnotched concrete beams, Int. J. Numer. Anal. Meth. Geomech. 37 (10) (2013) 1434–1452.